Implementation of Exhaust Gas Recirculation for Double Stage Waste Heat Recovery System on Large Container Vessel

Morten Andreasen[a,*], Matthieu Marissal[a,b,*], Kim Sørensen[a], Thomas Condra[a]

[a] *Department of Energy Technology, Pontoppidanstræde 101, DK-9220 Aalborg, Denmark*
[b] *EPF Ecole d'Ingenieurs, 3 bis rue Lakanal, 92330 Sceaux, France*

Abstract

Concerned to push ships to have a lower impact on the environment, the International Maritime Organization are implementing stricter regulation of NO_x and SO_x emissions, called Tier III, within emission control areas (ECAs). Waste Heat Recovery Systems (WHRS) on container ships consist of recovering some of the waste heat from the exhaust gas. This heat is converted into electrical energy used on-board instead of using auxiliary engines. Exhaust Gas Recirculation (EGR) systems, are recirculating a part of the exhaust gas through the engine combustion chamber to reduce emissions. WHRS combined with EGR is a potential way to improve system efficiency while reducing emissions. This paper investigates the feasibility of combining the two systems. EGR dilutes the fuel, lowering the combustion temperature and thereby the formation of NO_x, to reach Tier III limitation. A double stage WHRS is set up to reach the highest possible combination of pressure and temperature, and adapted to Tier III by introducing two alternative superheaters. The system design is optimized and found capable of producing from 400 to 1900 kW, with a weighted average power of 958 kW. The consumption profile is found to significantly impact the weighted average power, while the operation distribution between Tier III and Tier II (outside ECAs) has a much smaller influence. Furthermore, it is found that the low pressure should be kept near minimum, while the optimum high pressure increases from 7 to 12 bar with the load. By increasing the efficiency of the overall system, the CO_2 emissions can be reduced. The addition of a third cycle, used only in Tier III, is investigated. While increasing the total heat exchanger areas by approximately 40%, the cycle is found to increase the power production in Tier III operation by an average of 15%, and up to 50% at full load.

Keywords: Waste Heat Recovery, Exhaust Gas Recirculation, Tier III, Container Vessel, Steam Cycles, WHRS Model

1. IMO Regulations

Container ships are the most commonly used mean of intercontinental cargo freight. Due to the vast size of these ships, the amount of energy required for transport is similarly large. Increased focus on environmental issues, and the will to be part of a sustainable change have pushed the International Maritime Organization (IMO) to put regulations in place to lower the environmental impact of large container vessels.

1.1. Challenges of ship transportation

Ship freight traffic has increased significantly for the last decades, corresponding to the demand and will likely continue to grow since the demand for transport capacities has increased by about 7% every year for the last 20 years [1]. Three main issues have pushed owners and designers to improve the ship performances:

- Transport costs: Even if a larger ship will consume more energy, increasing the capacity will reduce the specific costs ($/mile/ton) .
- Fuel cost increase: The increase of fuel prices and the large consumption of large container ships have made it important to optimize en-

*Corresponding author
**Project Supervisor
Email addresses: mortenlandreasen@gmail.com (Morten Andreasen), matthieu.marissal@gmail.com (Matthieu Marissal)

ergy savings (i.e. minimizing the fuel consumption).

- Environmental impacts: The large consumption of those ships implies significant emissions of CO_x, SO_x and NO_x. International conventions and regulations make it mandatory for ships to reach certain levels of emission before they are allowed to travel. Some countries have limited the access to their national seas to ships complying with the strictest regulations.

1.2. CO_2 concern

CO_2 emissions have become a major focus point for most transportation related companies, since they have a large impact on global warming. To address it the IMO has established an index called EEDI that evaluates the amount of CO_2 emitted as function of the capacity and age of the ship [2]. It is required for any ship to comply with these limitation to sail. A Waste Heat Recovery System is often used to improve the overall efficiency of a ship. By generating on-board electricity, it reduces the fuel consumptions of the auxiliary engines, thereby reducing CO_2 emissions and reducing fuel costs [3].

1.3. NO_x and SO_x concern

NO_x and SO_x are not greenhouse gases. However, they are of importance since they have a large impact on the surrounding environment by leading to acid rain. To prevent such emissions, the IMO has set a number of emission limits with the MARPOL convention. Two of these are the Tier II and Tier III regulations. The condition Tier III is applied in ECAs, which are geographical areas located along the coasts of signatory countries. Soon the North Sea, North American coast, Mediterranean sea and part of Japan should be considered as ECAs. Going from Tier II to Tier III conditions implies a drastic reduction of NO_x and SO_x. NO_x emission limits are shown in Figure 1.[4][5]

While the SO_x concern can be addressed by the use of a higher quality fuel containing less Sulfur, or by the use of a scrubbing system, the NO_x emission reduction of around 70% will require the use of an additional system. Exhaust Gas Recirculation (EGR) can be used to lower the NO_x emissions by recirculating a part of the exhaust gas back into the combustion chamber.

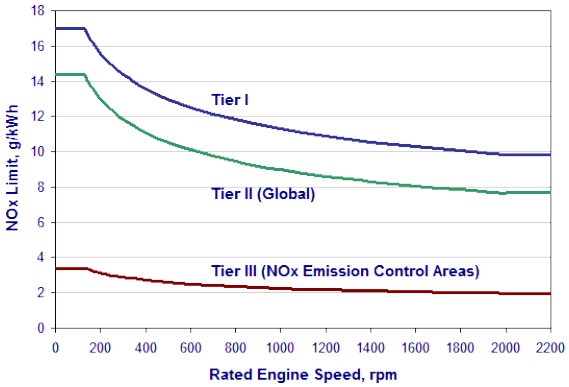

Figure 1: NO_x emissions limitation from MARPOL convention.[4]

2. Fuel and Combustion Model

The WHRS will recover energy from the exhaust gas. Knowing its composition is therefore required to evaluate its thermodynamic properties. Moreover, they are also required for they can demonstrate the impact of EGR and other parameters on the NO_x emissions. The combustion is modeled by using Cantera [6] software linked with MATLAB [7]. The exhaust gas properties are then determined by using REFPROP [8].

2.1. Fuel Model

The ships considered use Heavy Fuel Oil (HFO). According to the norm ISO 8217, HFO is: *A residual oil from distillation and/or the cracking system of natural gas processing and serves as fuel for marine diesel engines*[9]. The HFO category includes both finished products and the primary refinery streams from which they are blended. It is highly viscous and may contain some unwanted residuals. The chemical composition is therefore not exactly known and might differ from fuel to fuel.

HFO composition is complex to determine. However, using a statistical method [10], the mass fraction of chemical constituents can be calculated as follow:

$$\gamma_C = 0.64241 + 0.00505 \cdot LHV \quad (1)$$
$$\gamma_H = -0.22426 + 0.00826 \cdot LHV \quad (2)$$
$$\gamma_O = 0.27603 - 0.00628 \cdot LHV \quad (3)$$
$$\gamma_S = 0.30582 - 0.00702 \cdot LHV \quad (4)$$

Nitrogen, due to the low concentration in the fuel (lower than 0.34%) is neglected. Considering an

Lower Heating Value (LHV) of 42 $\frac{\text{MJ}}{\text{kg}}$ [3], the mass fraction of each components of the fuel can be determined. Relating the mass fraction to the number of atoms, the chemical composition of the HFO can be written as $C_1H_{1.54}O_{0.02}S_{0.01}$. It has to be noted here that the composition is evaluated per atom of carbon. The corresponding molar weight of fuel will be 14.18 kg/kmol.

The fuel will be mixed with air and then burned. The main stoichiometric chemical equation is shown in Equation 5 [11].

$$C_1H_{1.54}O_{0.02}S_{0.01} + 1.395 \cdot (O_2 + 3.76N_2) \rightarrow CO_2 + 0.77 \cdot H_2O + 5.2452 \cdot N_2 + 0.01 \cdot SO_2 \quad (5)$$

2.2. Combustion Model

The combustion is to be modeled in order to find accurate thermodynamic properties. Since no mechanism was found containing the exact fuel composition calculated, a combination of smaller known fuels is used to obtain a similar combustion. The selected mechanism would have to contain all of these smaller fuels. Additionally sulfur radicals are needed to evaluate the impact of various parameters on SO_x emissions. The Glassman mechanism [12] was found to comply with these two conditions. It was assumed that the HFO could be modeled with a combination of smaller fuels by fitting the LHV, the carbon/hydrogen and carbon/oxygen ratio. Moreover, it was assumed that the sulfur could be added as a fourth component.

Table 1 shows the fuel combination elected for the model.

Fuel	LHV	C/H	C/O	Mole Fraction
Methanol	19.92	1/4	1/1	0.2078
Acetylene	48.28	1/1	-	0.7489
Propane	46.34	3/8	-	0.0433
Average/Total	42.0	1/1.54	1/0.02	1

Table 1: Modeled fuel composition.

The resulting specific heat at constant pressure is found to be 1.68 kJ/kg·K, which is consistent with data on fuel properties for heavy diesel in gaseous phase (1.7 kJ/kg·K) [13].

The amount of excess air used during the combustion will depend on the load. Due to the occurrence of cross-over flow when the exhaust gas is pushed out of the combustion chamber, some of the air does not participate in the combustion. From MAN data in Tier II conditions, an average excess air ratio of 3.75 has been chosen. The combustion was modeled at equilibrium conditions, considering a pressure of 140 bar and a temperature of 800 K. The exhaust gas composition found is shown in Table 2. This is without considering dissociation.

Molecule	Mass Fraction
Ar	0.0097
CO_2	0.0403
N_2	0.7700
O_2	0.1500
H_2O	0.0298
SO_2	0.0002
Total	1.0000

Table 2: Exhaust gas composition computed with Cantera.

3. EGR and NO_x emission

3.1. Exhaust Gas Recirculation

EGR consists in recycling a part of the exhaust back to the combustion chamber to lower the amount of NO_x emissions. The EGR is quantified by a percentage which can differ from source to source. Here, the EGR rate will correspond to the amount of exhaust recirculated over the total intake of the combustion chamber (i.e exhaust gas, air, fuel). The EGR rate is shown in Equation 6.

$$EGR(\%) = \left(\frac{\dot{m}_{EGR}}{\dot{m}_i}\right) \cdot 100 \quad (6)$$

The amount of EGR has been assumed as optimized and given by MAN Diesel&Turbo and is not constant, with lower percentage of exhaust being recirculated for higher load as shown in Figure 2.

3.2. NO_x kinetic and emissions

The main mechanisms of NO formation have been studied extensively in the literature. It is commonly accepted that in combustion of fuel involving Nitrogen, the *Zeldovich* mechanism shown in Equation 7 and 8 extended with the *Lavoie et al.* mechanism shown in Equation 9 can be used to describe NO formation [11].

$$O + N_2 \rightleftharpoons NO + N \quad (7)$$

$$N + O_2 \rightleftharpoons NO + O \quad (8)$$

$$N + OH \rightleftharpoons NO + H \quad (9)$$

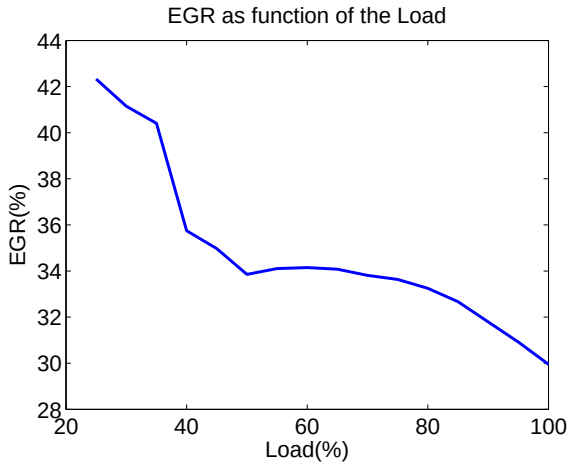

Figure 2: Recirculation percentage as function of the load.

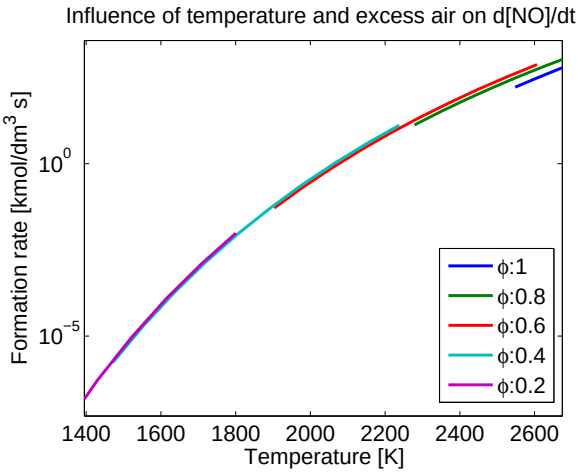

Figure 3: NO formation rate for various adiabatic flame temperatures and excess air ratio.

By using these equations and the related kinetics of NO formation, Equation 10 can be found. Calculations are described more extensively in [13].

$$\frac{d\,[NO]}{dt} = \frac{6 \cdot 10^{16}}{T^{0.5}} exp\left(\frac{-69090}{T}\right) [O_2]_{eq}^{0.5}\,[N_2]_{eq} \tag{10}$$

From Equation 10 it can clearly be seen that the NO kinetic will be influenced by the amount of Oxygen and Nitrogen present during the combustion. However, it can also be seen that temperature will have a major impact on the NO formation, with lower temperature leading to slower NO production.

The influence of the temperature is illustrated in Figure 3, where the NO formation kinetic is shown as a function of the equivalence ratio and the adiabatic flame temperature. Lowering the equivalence ratio increases the quantity of air in the chamber, and thereby allows lower flame temperatures.

Recirculating exhaust gas will both increase the mass in the combustion chamber, and increase the c_p value of the mixture, thereby lowering the temperature. This will lead to lower NO_x emissions as illustrated in Figure 4, where the NO mole fraction is shown as function of the rate of EGR. It will also have an impact on NO_2 formation, but with the concentration being around 10 times lower than the NO, it has not been taken into account. Figure 4 shows that EGR has the capacity of lowering the NO emissions by a factor of 10, by going from 10 to 50 %.

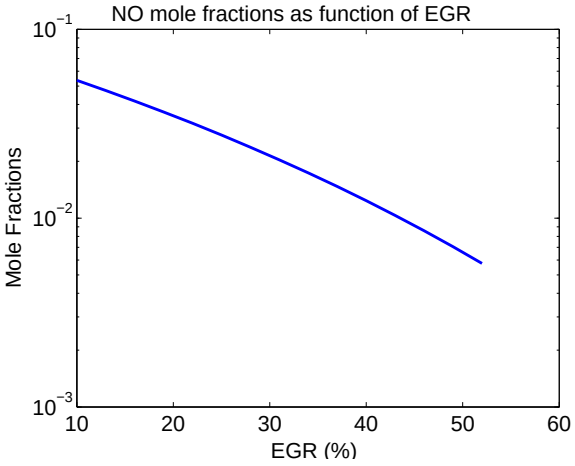

Figure 4: NO mole fraction as function of the EGR(%).

4. Double-Stage Waste Heat Recovery

The Waste Heat Recovery System drains energy from the exhaust gas. Two steam cycles are preheated using the jacket water and scavenge air. The cycles are then evaporated and superheated in the stack before being sent through a steam turbine to generate electricity.

The process in demonstrated in a T-s diagram in Figure 5, where T is the temperature and s is the specific entropy.

4.1. Exergy

Exergy is a measure of potential work in a substance. This can principally include any kind of energy transfer. In thermodynamics, exergy can be

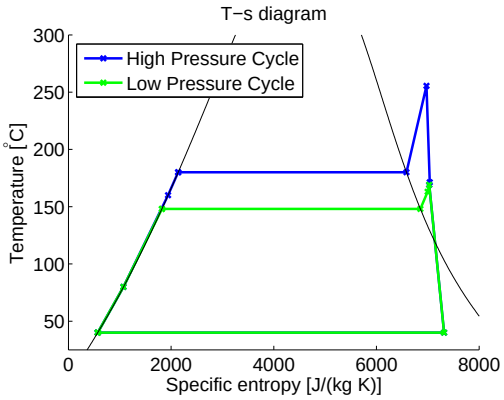

Figure 5: T-s diagram.

interpreted as a unit of steam quality. Equation 11 shows the expression used for the specific exergy ψ, with the velocity term left out, since this becomes negligible [14]. h and s are specific enthalpy and specific entropy respectively, while T is the temperature. Subscript 0 denotes a reference state.

$$\psi = (h - h_0) - T_0(s - s_0) \tag{11}$$

Figure 6 shows the development of specific exergy with temperature and pressure. It can be seen that while increasing pressure does increase specific exergy, this effect diminishes quickly. Specific exergy also increases with temperature, for which reason a fluid should be heated as high as possible in a steam cycle. Consequently, a high temperature heat source, such as the EGR string, should be used as the final source of superheating.

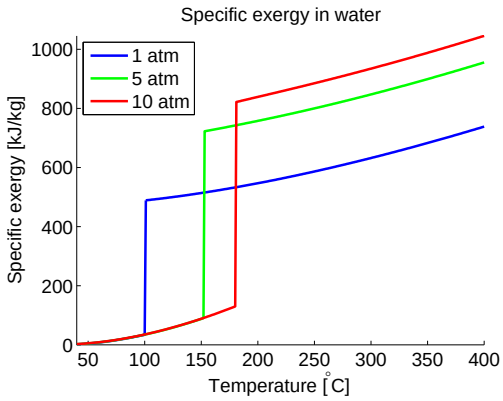

Figure 6: Developement of Specific exergy with temperature.

4.2. Heat Sources

Figure 7 shows the available heat sources for the WHRS during normal (Tier II) operation.

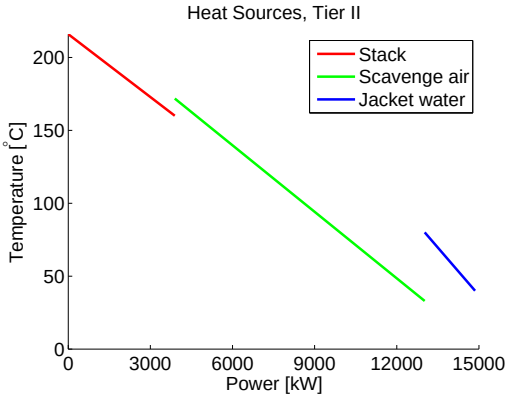

Figure 7: Tier II heat sources.

Notably, while the scavenge air represents the largest quantity of energy available, the temperature of the stack is higher, making it more useful and more worth extracting.

Figure 8 shows the available heat sources for the WHRS during operation inside ECA's (Tier III) operation.

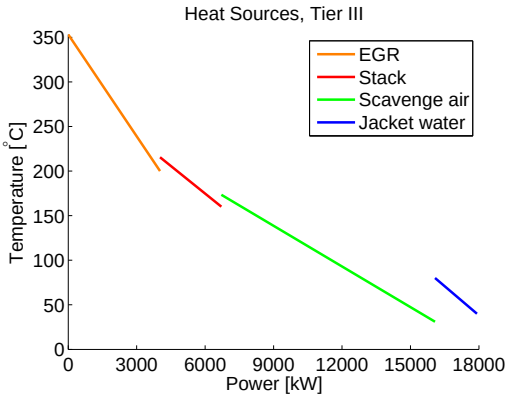

Figure 8: Tier III heat sources.

Not only does the recirculated exhaust gas represent a larger amount of available energy than the stack, it is also of a higher temperature. Therefore, the EGR string should be the final sources of heat used before the cycle fluid reaches the steam turbine. The complete used system is shown in Figure 9.

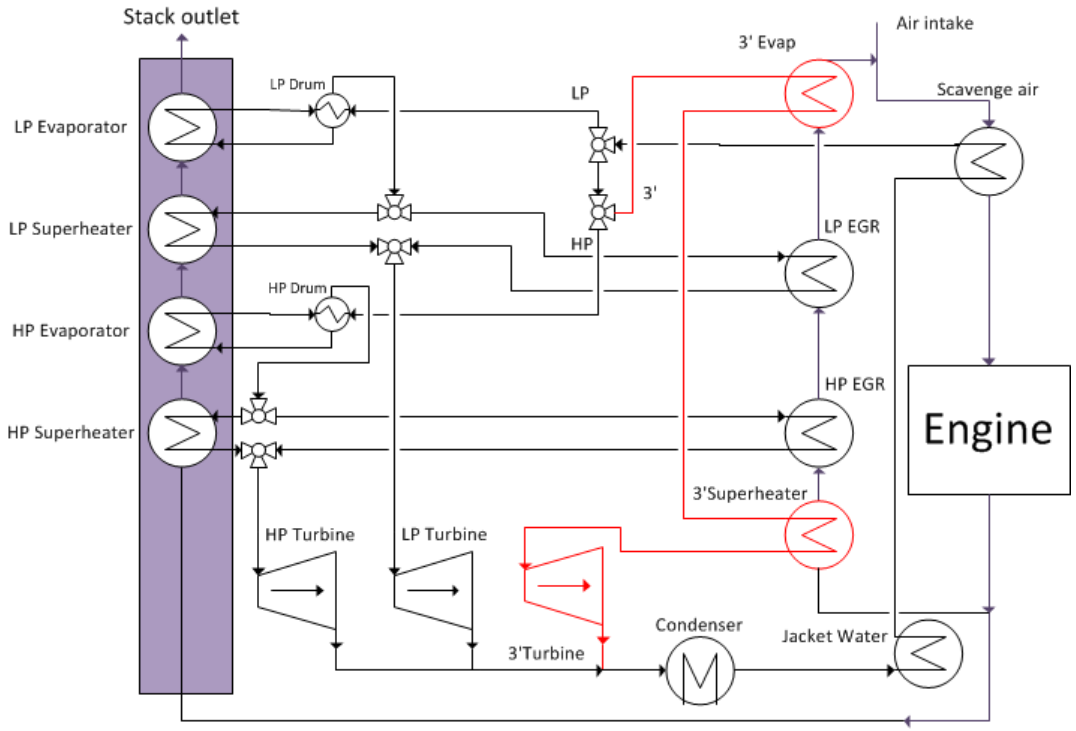

Figure 9: System schematic. The initially investigated 2-stage system is shown in black. For the later investigated 3rd cycle, the red components are added.

5. WHRS Model

To model the power production of the WHRS at all engine loads, two system characteristics must be established, One characteristic being the heat transfer capability of the heat exchangers in the system (here represented by an area and constant heat transfer coefficient) and the other being the turbine constant.

The turbine constant is found from Stodola's Law shown in Equation 12 [15].

$$C_T = \dot{m}\sqrt{\frac{p_{in}v_{in}}{p_{in}^2 - p_{out}^2}} \tag{12}$$

The heat exchanger areas are approximated from desired temperatures and a reasonable overall heat transfer coefficient, using the log mean temperature difference method.

5.1. Design Model

The outline of the design model is shown in Figure 10. The model takes design pressures for the HP and LP cycle. The temperatures in the preheaters are defined by the heat sources. The high pressure section of the stack is calculated first, and the low pressure section is then defined by the remaining energy in the exhaust gas. The cycle mass flows are then found, and used to calculate heat exchanger areas with the LMTD method. The mass flows are also used when the turbine constants are calculated with Stodola's law after having applied turbine efficiencies. The model is set up using MATLAB[7].

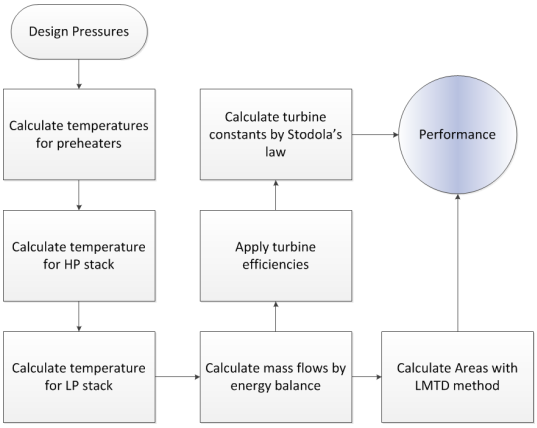

Figure 10: Design model flowchart.

5.2. Partload Performance Model

In the performance model, the outlet properties of the fluids are calculated with the NTU (Number of Transfer Units)- method, using the previously found heat exchanger areas. The mass flow of the system is further limited by Stodola's Law (Equation 12), which is now used with the found turbine constants to evaluate the turbine mass flow, given the operation pressure. The model now uses a partial engine load, the pressures of the HP and LP cycles, and the characteristics calculated in the design model. Here, the mass flows are initially guessed, and then re-evaluated when fluid properties have been calculated. Temperatures after each component are calculated with the NTU method. The process runs until the mass flows converge, before calculating the powers of the turbine at that particular load.

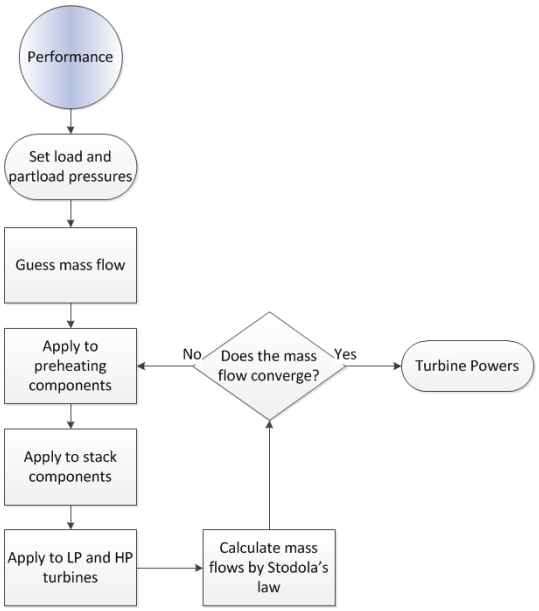

Figure 11: Partload performance model flowchart.

6. Optimization

To avoid extensive economic considerations, the heat exchangers are limited to be designed with a pinch of 10 K. The target variables of the optimization are therefore the input design pressures.
Since the heat exchanger areas and turbine constants are not the only variables in the performance model, the part-load pressures must be optimized for each load and for each configuration. This is done in an embedded performance optimization. The overall procedure is as follows:

1. Guess design pressures
2. Calculate aras and C_T
3. Optimize performance
   (a) Guess operation pressures
   (b) Calculate mass flows and turbine powers
   (c) Adjust operation pressures
   (d) Go to (b), repeat until convergence
4. Calculate objective function
5. Adjust design pressures
6. Go to (2), repeat until convergence

To account for both loads, and to account for the disparity between operation in Tier II and Tier III, the objective function in Equation 13 is used for the overall optimization. LR represents the load repartition, while the 0.7 and 0.3 are the repartition between Tier II and Tier III operation.

$$P_{WHRS} = \sum^{load}(0.7 \cdot LR_{T_{II}} \cdot P_{T_{II}} + 0.3 \cdot LR_{T_{II}} \cdot P_{T_{III}}) \tag{13}$$

To avoid material concerns, maximum allowable pressure is set to 15 bar (at significantly higher pressures, reinforced components would be required [10]). The low pressure boundary is set to avoid the exhaust gas being cooled below condensation temperature, which would result in the formation of sulfuric acid in the chimney.

$$3.5bar < p_{LP} < p_{HP} < 15bar \tag{14}$$

In addition to the limitation in Equation 14, the operation pressures cannot exceed the design pressure.

$$p_{HP\ operation} <= p_{HP\ design} \tag{15}$$

$$p_{LP\ operation} <= p_{LP\ design} \tag{16}$$

While the embedded performance optimization can be carried out with a Hessian-based solver, the overall design optimization is too unstable, and is optimized with a genetic algorithm. The optimal design pressures are 12.14 and 4.41 bar for the high- and low pressure cycles respectively. The optimal performance pressures are shown in Figure 12.
The power production at optimum pressures is shown in Figure 13. At higher loads, the exhaust gas contains more energy. To transfer the additional energy to the cycle, the cycle mass flows must

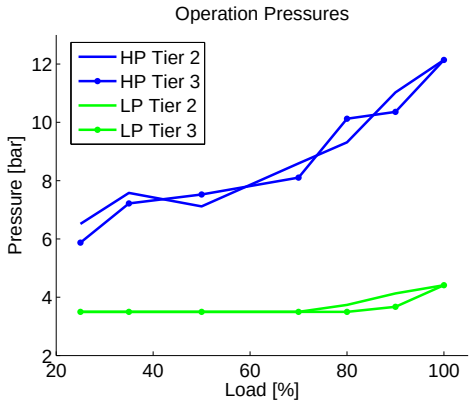

Figure 12: Optimal performance pressures.

increase, and the pressures must grow accordingly to respect Stodola's Law (Equation 12).
The optimum pressures therefore increase with the engine load until they reach the design pressures at full load.

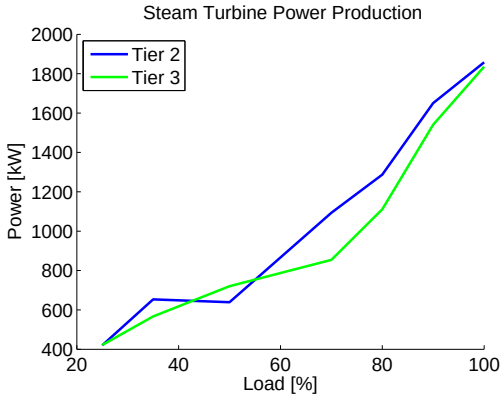

Figure 13: Power Production.

7. 3rd Cycle

7.1. Efficiency Analysis

To determine how much unrecovered energy is left in the stack, an exergy efficiency is defined as seen in Equation 17. Exergy efficiency represents the ratio of recovered energy to the recoverable energy, excluding preheating[16][17].

$$\eta_\psi = \frac{\eta_{WHRS}}{\eta_{\psi-max}} = \frac{P_{Turbines} - P_{pump}}{m_{eg}\psi_{eg}} \qquad (17)$$

The exergy efficiency is shown in Figure 14 for the optimized 2-cycle system for all loads. It can be seen that while the Tier II operation ranged between 65% and 95%, Tier III stays just above 40%. This is because a large part of the energy in the exhaust gas recirculation string is not utilized.

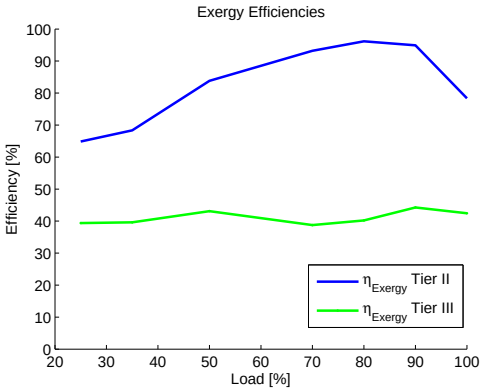

Figure 14: System efficiencies.

7.2. Additional Cycle

To fully utilize the remaining power in the exhaust gas recirculation string, an additional cycle, exclusive to Tier III operation, is introduced. This cycle will be set at 15 bar, and will superheat at the EGR inlet. The cycle fluid will evaporate in the EGR string after the superheaters of all three cycles, just before the EGR is re-introduced into the engine. The third cycle is shown in red on Figure 9.

The resulting optimized power production is shown in Figure 15. While the Tier II production remains unchanged, production in Tier III has increased to peak at almost 3000 kW. The system now operates more efficiently in Tier III operation than in Tier II.

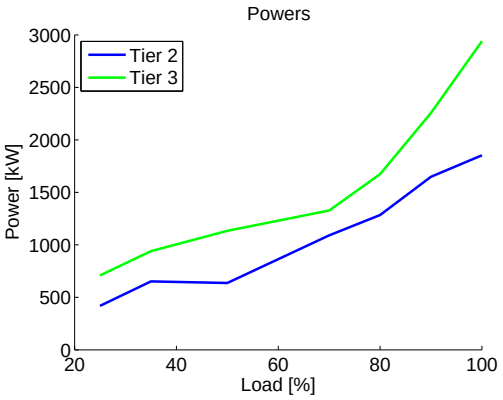

Figure 15: Third cycle power production.

Since an additional evaporator is a much larger component than an additional superheater, changes to the overall system size will be more prominent. Moreover, another turbine may be required for the third cycle, as well as another condenser, extra pipework, valves, etc.
No economic study has been made, but rough calculations estimate a total increase in heat exchanger areas of approximately 27% compared to the originally proposed 2-stage system. This does not include the potential need for an additional turbine, which would further increase the system cost. The maximum obtained steam turbine power production is increased by almost 1 MW, but the weighted average power production (Equation 13) is increased by 15-18%.

8. Conclusion

To evaluate the influence of exhaust gas recirculation on a waste heat recovery system, the chemical composition of the exhaust gas was studied. It was found that the composition of the fuel could be averaged to $CH_{1.54}O_{0.02}S_{0.01}$. Its combustion could be adequately modelled using the Glassman mechanism, and a mixture of three small known fuels, with the same average chemical composition and LHV as the evaluated HFO.
NO_x emissions have been shown to be highly dependent of the combustion temperature. It was found that re-introducing part of the exhaust gas to the combustion chamber would significantly reduce the combustion temperature due to the higher c_p value of the exhaust gas. This has been shown to reduce NO_x emissions sufficiently to comply with Tier III operation.
Even considering the massive reduction in NO_x particles after combustion, the thermodynamic properties of the exhaust gas were found to be nearly identical with or without EGR.
A double stage waste heat recovery system was used to regenerate heat from the exhaust gas. A brief exergy study revealed better theoretical results with higher temperatures rather than higher mass. Accordingly, the heat sources were arranged to maximize the the final temperature of each steam cycle. The WHRS model was split into a design and a partload performance model, with the main difference between them being a change from the LMTD to the NTU method for the heat exchangers, and a re-arrangement of Stodola's law for the steam turbines.
Operating a standard 2-stage WHRS with the EGR cycle, it was found that the system could produce up to 2 MW of electrical power, and that with the addition of two alternative superheaters in the EGR string, Tier III production could be kept near that of Tier II.
An exergy analysis revealed a large quantity of available power still present in the EGR string, and an additional steam cycle was proposed. Due to the vast size of the evaporator relative to the extra superheaters, as well as the possible need of a third turbine and additional condenser, this represents a much larger investment. However, it was found that the implementation of an additional high pressure cycle in the EGR string could increase steam turbine production in Tier III to almost 3 MW.

9. Acknowledgments

The Authors would like to thank MAN Diesel&Turbo Copenhagen for their help and support with both concrete data and general know-how during the course of the project. Especially Bent Ørndrup Nielsen, Senior Researcher, and Kari Anne Tveitaskog, Marine Engineer, who had the kindness and generosity to help us all along our project.

References

[1] A. S. G. . C. KG, Global Maritime Trade on Course, Esplanade 23, 20354 Hamburg, Germany.
URL http://www.auerbach-schifffahrt.de/en/knowledge/
[2] IMO, Guideline on the method of calculation of the attained energy efficiency design index (EEDI) for new ships (2012).
[3] MAN Diesel&Turbo, Waste Heat Recovery System (WHRS) for reduction of fuel consumption, emissions and EEDI (December 2012).
[4] IMO, Nitrogen Oxides - Regulation 13, International Maritime Organization (2013).
[5] IMO, Sulphur Oxides (SOx) - Regulation 14, International Maritime Organization (2013).
[6] Cantera, Cantera version 2.1.1 (2012).
URL http://cantera.googlecode.com
[7] Mathworks, Matlab is a product of the mathworks, inc., matLab is a product of The MathWorks, Inc. (2014).
[8] M. M. E.W Lemmon, M.L Huber, Refprop version 9.0, national Institute of Standards and Technology, U.S. Department of Commerce (2010).
[9] ISO, Iso 8217:2012 petroleum products – fuels (class f) – specifications of marine fuels (2012).
URL http://www.iso.org/iso/home/store/catalogue_tc/catalogue_detail.htm?csnumber=50613
[10] T. Condra, Conversations with Thomas Condra, AAU (2013).

[11] S. R. Turns, An Introduction to Combustion, Concepts and Applications, McGRAW-HILL, 2000, iSBN: 0-07-230096-5.

[12] I. Glassman, Combustion, 3rd ed. (Appendix B), Academic Press, 1996, iSBN: 978-0-12-285852-9.

[13] J. B. Heywood, Internal Combustion Engine Fundamentals, McGRAW-HILL, 1988, iSBN: 0-07-100499-8.

[14] M. A. Boles, Y. A. Cengel, Thermodynamics, An Engineering Approach, 7th Edition, McGraw-Hill, 2011, iSBN: 978-007-131111-4.

[15] M. P. Nielsen, Analysis Of Advanced Thermal Process Systems, notes and Slides from mm1, AAU (2013).

[16] K. Chen, J. Wang, Y. L. Yiping Dai, Thermodynamic analysis of a low-temperature waste heat recovery system based on the concept of solar chimney, Energy Conversion and Management 80.

[17] W. Fu, J. Zhu, W. Zhang, Z. Lu, Performance evaluation of kalina cycle subsystem on geothermal power generation in the oilfield, Applied Thermal Engineering 54.